Flow Patterns in Wire-on-Tube Heat Exchangers Based on Various Low Refrigerant Mass Flow Rates

Louay Abd Al-Azez Mahdi
Energy and Renewable Energies Technology Center, University of Technology- Iraq

Mohammed A. Fayad
Energy and Renewable Energies Technology Center, University of Technology- Iraq

Miqdam T. Chaichan
Energy and Renewable Energies Technology Center, University of Technology- Iraq

https://doi.org/10.5109/7183366

出版情報：Evergreen. 11 (2), pp.872-886, 2024-06. 九州大学グリーンテクノロジー研究教育センター
バージョン：

Flow Patterns in Wire-on-Tube Heat Exchangers Based on Various Low Refrigerant Mass Flow Rates

Louay Abd Al-Azez Mahdi[1], Mohammed A. Fayad[1], Miqdam T. Chaichan[1*]
[1] Energy and Renewable Energies Technology Center, University of Technology- Iraq.

*Author to whom correspondence should be addressed:
miqdam.t.chaichan@uotechnology.edu.iq

(Received April 1, 2023; Revised March 21, 2024; Accepted April 7, 2024).

Abstract: A theoretical investigation of flow patterns inside a wire condenser tube was conducted for two refrigerants (R-600a and R-134a) with multiple mass flow rates. It is possible to determine the type of refrigerant flow pattern in this type of heat exchanger as well as the location of the change from one type to another using the proposed model. In this case, the flow patterns appear stratified (S), stratified-wavy (SW), plugged (PL), and slugged (SL). We (4-7) and Fr (2-5) in the quality range (0.80-0.4) showed the first change in the condensation flow pattern from stratified to stratified-wavy. A second flow change was observed at Fr (2-0.4) and We (4-2) for the quality range (0.15-0.05). Results for the refrigerant R134a and R-600a indicate that the condensing temperature of the refrigerant does not have an effect on the flow pattern.

Keywords: Two-phase flow; in-tube condensation; stratified; stratified–wavy; wire condenser.

1. Introduction

Around the world, house appliances like refrigerators and freezers are commonly used to preserve perishable products. With concerns over the environment due to the harm done by conventional refrigerants in cooling systems as reported by many researchers, studies into alternatives which are more environmentally friendly have escalated in the last few decades[1)2)3)4)]. The performance of these alternative refrigerants must first be investigated to identify their efficiency and effectiveness compared to the previous ones. R-600a and R134a being reported in this paper are amongst those refrigerants that are still being studied.

Condensing may be divided into a flow of shear forces and a flow of gravitational force. gravitational force control stratified flow (S) and stratified wavy flow (W-S), while shear forces control annular flow[3)5)6)]. Flow patterns are affected by heat transfer and flow processes. Therefore, the type of flow pattern is dependent on the rate of flow, quality and properties of the medium in order to get right calculation for heat dissipation for the wire on tube heat exchanger. This includes the type of liquid or refrigerant, as well as the inner tube diameter.

Mass flow rate of refrigerant represents mass velocities, and mass velocity together with quality determines the predominant flow pattern. The type of fluid is represented by thermophysical properties and the inner tube diameter. Thermal properties such as density, viscosity, the ratio between these quantities and surface tension can be determined by Froude number (Fr) and Weber number (We). When the mass flow is low, stratification occurs. The condensation is formed by film-wise condensation that drains from the top towards the bottom under gravitational force. Previous work stated that stratified flow was observed only in small inner diameter tubes with low mass velocities. The change in the flow pattern is caused by the instability of liquid and vapor velocities due to the overlap between the vapor and the fluid flow, previous studies in the literature have focused on condensation heat transfer. This is due to the necessity to choose a suitable heat transfer coefficient equation[7)].

Many researchers produced a map to view the type of the flow pattern in side tube for condensation process;

Taitel and Dukler [8)] predicted the flow regime model and map of horizontal gas-liquid flow. They identified five types of flows: smooth stratified (SS), stratified-wavy (SW), intermittent (I), slug (SL), plug (PL), annular (A), bubble (B). Also, they obtained five dimensionless groups which represent the transition. The flow regime criteria were used to investigate condensation in pure refrigerants in the horizontal tube as reported in the study by Breber et al. [9)]. The study is based on two parameters: the first parameter represents the relationship between the shear forces and the gravitational force on the condensate film which represents the Wallis dimensionless gas velocity, and the second parameter is

the ratio of vapor to liquid volume which represents the Martinelli parameter. Table 1 lists the conclusions of the above study.

Table 1. Limitations of Breber et al.[9)]

Flow type	dimensionless Wallis gas velocity (J_g^*)	parameter of Martinelli (Xtt)
Wavy(W) or stratified(S)	< 0.5	<1.0
Intermittent(I)	<1.5	>1.5
Annual(A)	>1.5	<1.0
Bubble(B)	>1.5	>1.5

Biphasic flow diagram for condensing in horizontal tubes was found by Tandon et al.[10)]. The working fluids used in the above study were R-12 and R-113 and the diameters of the tubes were 4.8 mm to 15.9 mm as well as the length of the tubes was 0.61 m and 4.42 m. In order to obtain flow patterns, Wallis dimensionless gas velocity and void fraction were applied, and the limitations of this study were presented in Table 2.

Table 2. Limitations of Tandon et al.[10)]

Flow type	Wallis dimensionless gas velocity J_g^*	a void fraction $\frac{1-\alpha}{\alpha}$
Spray (Sp)	≥ 6	≤0.5
Annular (A)and semi-annular (SA)	$1 \leq J_g^* \leq 6$	≤0.5
Wavy (W)	≤1	≤0.5
Slug (SL)	$0.01 \leq J_g^* \leq 0.5$	≥0.5
Plug (PL)	≤ 0.01	≥0.5

Nitheanandan et al.[11) 12)] studied the We and Fr numbers to determine the type of condensation flow pattern. A suitable equation to represent the heat transfer coefficient of a mist (M), annular (A), and wavy (W) flow. The study mass velocity was 4 to 305 (kg.cm^{-2}. s^{-1}). The study didn't refer to stratified or stratified-wavy flow which may be included with wavy or these types of flow patterns did not appear in the study.

Nitheanandan et al.[11)] examined the type of inside condensation flow pattern according to the We number and Fr number. It was found that the appropriate equations to represent the heat transfer coefficient of M, A, and W flows could be used. In Table 3, we present our conclusions and limitations.

Table 3. Limitations of Nitheanandan et al.[11)]

Flow type	We	Fr	$\frac{x^2G^2}{\rho_g}$ (kg.m^{-1}.s^{-2})
Mist (M)	≥40	≥7	>100
Annular (A)	<40	≥7	>100
Transition from wavy annular to wavy (WA-W)	-	=18	-
Wavy (W)	-	<7	-

The condensation inside the tube was also studied by Dobson and chato.[13)]. Flow patterns in two phases are split into two types: gravity flow and shear flow. The study found heat transfer correlation for different flow patterns depending on Reynolds number, Nusselt number, Fr and Martinelli parameter.

Two-phase flow is determined by mass velocity, flow rate, and the quality of the vapor as presented by El Hajal et al.[5)] and Thome et al.[14)]. They studied the effect of the refrigerant type on the transition areas. Based on data from previous studies[8) 9) 10)], Revised equations for the void equation, mass velocity, and heat transfer coefficient were obtained. In addition, the study modified the Kattan map in order to be used for condensation. The main limitations of this study are presented in Table 4.

Table 4. Limitations of El Hajal et al.[5)] and Thome et al.[14)].

Flow type	limitations
Annular	$G > G_{wavy}, G < G_{mist}, \quad x > x_{IA}$
Intermittent	$G > G_{wavy}, G < G_{mist}$ or $G < G_{bubbly}, x < x_{IA}$
Stratified-wavy	$G_{strat} < G < G_{wavy} \quad fully\ stratified\ if\ G < G_{strat}$
Fully stratified	$G < G_{strat}$
Mist	$G > G_{mist}$

Jung et al. has previously investigated flow condensing within the horizontal plain tubes[15)]. The heat transfer coefficient was found using several refrigerants. Also, the study covered mass fluxes of 100–300 kg s^{-1} m^{-2} at 40°C saturation temperature with inner diameter and length of test tube of 9.52 mm and 1 m, respectively. Besides, the study modified coefficients of heat transfer were calculated using the Dobson correlation [13)].

The penalty factor was described by a two-phase condensation heat transfer for annular flow by Cavallini et al. [16)]. In this study, the analysis depends on the tube diameter, saturation temperature, and quality of the tube (0.5). There are two temperature differences that

contribute to the penalty factor: the temperature difference between the refrigerant and the inner wall of the pipe must be considered in the first case. Secondly, it is important to consider the temperature difference between entering and leaving the system when refrigerant is entering. In the first temperature difference, heat transfer coefficients are considered, while in the second, pressure drop affects the temperature difference.

Koyama and Yonemoto[17] experimentally studied two-phase flow into a smooth pipe of diameter of 7.5 mm and 1024 mm length, and micro-fin tubes with diameters and lengths of 8.86 mm and 1015 mm, respectively. In this study, the working fluid was R-134a and predicted the void fraction and compared it to previous correlations.

To calculate the heat transfer coefficients of pure and zeotropic refrigerants, Thome [18] and DelCol et al.[19] A model for a two-phase flow structure was developed. The model is dependent on the gravity and shear regimes of flow. A novel two-phase flow pattern appeared along with convection condensation heat transfer equations. The study depended on El Hajal et al. [5] and Thome et al. [14].

Jassim et al. [20] used probabilistic techniques to measure and discover the type of condensation flow patterns by creating a supplementary two-phase flow condensation map. The approach demonstrated good agreement with the experimental data for R-134a in a horizontal tube of 8.92 mm inner diameter.

Suliman et al.[21] examined the condensing of R-134a in a horizontal smooth copper tube. The diameter of the tube is 8.38 mm and its length is 1.546 m. It covers a mass flux range of 75-300 kg s^{-1} m^{-2}. In this experiment, the saturation temperature was 40°C and the vapor quality was between 0.76 and 0.03. According to El Hajal et al.[5] and Thome et al.[14], this study was based on previous research.

The work concerned the transitional line between SW and annular (A) flow. The results of this study showed that stratified flow was strongly influenced by temperature differences.

The condensation of R-410A, R-22, and R-134a inside a horizontal small copper tube was investigated by Son and Lee[22]. Furthermore, the inside diameters were 5.35, 3.36, and 1.77 mm and the lengths were 1220 mm, 2660 mm, and 3620 mm. In the study, mass fluxes ranged from 200 to 400 kg s^{-1} m^{-2} at saturation temperature 40°C. Taitel and Dukler[8] map was used to test the data in order for determining the kind of flow. In the study, the focus was on a small tube diameter which are not covered by previous studies. Studies have shown that heat transfer coefficients increase with decreasing inner tubes.

Van Rooyen et al.[23] Predicted the two-phase flow in smooth horizontal copper tubes using probabilistic time-fraction flow. The inside tube diameter was 8.53 mm and working fluid is R-22 and R-134a. The study covers the range 200-700 kg s^{-1} m^{-2} mass flux. The study used friction time to classify the flow regime. The theoretical part of the study based on Thome et al.[14].

Transfer of condensate heat through horizontal channels was studied by Lee et al.[24]. Two models were applied to measure heat transfer. The study used video capture to view the behavior of interfacial condensation film. The tests covered four types of flow regime: S, SW, W-A, and A. The working fluid used was FC-72 covering mass velocity of 33.4, 49.2, 65.6, 83, and 115.8 kg s^{-1} m^{-2}. Study limitations are outlined in the table 5.

Table 5. Limitations of Lee et al.[24]

Flow pattern	limitations
plug	We ≤ 5
stratified - wavy	We ≤ 10
annular	We ≥ 20
mist	We ≥ 30

Mohseni et al.[25] Analyzed the heat transfer and condensation flow of R-134a within a smooth tube from various angles. According to the results, the inclination increased the heat transfer coefficient.

In an article published by Doretti et al.[26] a brand-new condensation map was discovered. In order to achieve this, the authors used visual and experimental testing, previous studies, and correlations of the heat transfer coefficient between the two phases. Tests were conducted in an 8 mm diameter tube and the refrigerant's mass velocity was inspected between 100 and 900 kg s^{-1} m^{-2}. Several groups reviewed the results of the study, including Taitel and Dukler[8], Breber et al.[9], Tandon et al. [10], and El Hajal et al.[5] and Thome et al.[14]. The results showed that the flow profile with low mass velocity depended on the refrigerant temperature differential from the wall.

Using experimental analysis by Park et al.[27], completed an experimental analysis on the condensing fluid Fluc-72 in horizontal tubes of diameter of 10.16 mm and a length of 1219 mm, which was used to observe gravity effects on S, SW, W-A, and without gravity on W-A flow patterns. The study showed that the annular film type is dominated by share flow type not depending on gravity with increasing tube length, the heat transfer coefficient decreases steadily from the inlet due to the growing of thickening film of liquid updated new limitations for transient line as presented in Table 6.

Table 6. Limitations of Park et al.[27)]

Flow type	Weber number (We)	Modified superficial vapor velocity J_g^*
(S) Stratified	We < 6.03	J_g^*<0.28
(S-WS) Stratified-wavy stratified	6.03 ≤ We ≤ 19.39	0.28≤J_g^*≤1.61
(WS-WA) Wavy-stratified to wavy-annular	19.39 ≤ We ≤ 25.46	1.61≤J_g^*≤2.54
(W-A) Wavy-annular	We ≥ 25.46	J_g^*≥2.54

The laser Doppler velocimetry was used by Saini et al.[28)] to studied the behavior of S to S-W flow. Part of the study considered the influence of superficial Reynolds numbers on gases and liquids. The other part of the study was to measure the fluctuations occurring near the air-shear interface. The inside tubes had diameters of 21 mm, 25 mm, and 50 mm and lengths of 14 m.

Sereda et al.[29)] studied the stratified flow condensation inside an ordinary 17 mm diameter tube. There was a range of quality of 0.95-0.23 and a saturation temperature of 40°C in the study. Groups of 12 refrigerants were used and covered the mass velocities 6-57 kg s^{-1} m^{-2}. In order to determine heat transfer, CFD was used.

Mahdi et al.[30)] theoretically analyzed the flow in the narrow tube. The study found the flow pattern was stratified when the mass velocity under 100 kg.sec^{-1}.m^{-2}.

Al-Zaidi et al.[6)] Various factors, including refrigerant mass flux, local vapor quality, coolant flow rate, and inlet coolant temperature, were investigated experimentally to determine the local condensation heat transfer coefficient.

The most relevant points can be summarized from the literature which refer to the flow pattern at low mass velocities:

The flow patterns in small diameter tubes differ from those in large diameter tubes due to the surface tension between the liquid and gaseous phases.

The effect of the inner tube diameter on the transient regime is still not clear.

The values of mass velocities are higher than 100 (kg. s^{-1}.m^{-2}).

Referring to Breber et al.[9)], S, S-W, W flows may be calculated when the wall is gas velocity dimensionless parameter 0.5 and the Martinelli parameter 1.0.

The S, S-W, W flow may be determined when the Froude number < 7.0 with reference to Nitheanandan et al.[11)] and Nitheanandan and Soliman[12)]. The stratified flow depends heavily on the temperature difference between the vapor and the tube wall temperature according to El Hajal et al.[5)] and Thome et al.[14)] and Doretti et al.[26)].

According to Son and Lee[22)], as the inner diameter decreases, the heat transfer coefficient increases. They studied the plug flow when We numbered 5 and the SW flow when We numbered 10.

The stratified, stratified-wavy, and wavy gravitational flows were studied in work by Park and Mudawar[27)]. A stratified flow occurs when We number > 6.03 and Wallis dimensionless gas velocity > 0.28. A stratified-wavy flow occurs when We > 6.03.

This aims of this study are: first investigation the type of refrigerant flow pattern at low mass velocities and find the location of the change of the flow from S to S-W and S_W to plug flow. Secondly, the effect of different refrigerant types, tube diameters, and condensing saturation temperatures on the flow pattern. Third the study plan to show the ability of using the non-dimensional groups like Fr number and We number to determine the transient rejoin from S to SW flow at the starting of condensation and from SW to PL or SL flow at the end of condensation.

2. Modelling and theoretical analysis

In order to analyze the theoretical model, the integration method for condensation inside the tubes of the wire condenser was applied with Equal Equations Solver software. The recommended sizes of inner diameters for wire condensers are 3.24 mm (3/16”), 4.826 mm (1/4”), and 6.299 mm (5/16”). These sizes were used because they are available commercially in the local markets. The refrigerant mass flow rates are 1, 1.5, 2.5, 3.25, 4,4 and 5.5 (kg/h) which correspond to the size of the compressor (1/12-1/3 hp) used in manufacturing refrigerators and freezer home appliances. The current analysis also depends on the limitations that are presented in Table (4) in the introduction.

The study was carried out using two refrigerants: R-134 and R-600a. R-134a possesses several advantages over its predecessors, The first two groups of these are chlorofluorocarbons (CFCs) and hydrochlorofluorocarbons (HCFCs)., including a lower environmental impact. There is no chlorine in it, which depletes the ozone layer. R-134a is compatible with copper and aluminum in refrigeration systems. As a result, existing systems can be retrofitted or replaced without significant modifications. Thermodynamic properties of R-134a make it ideal for refrigeration applications. It is also widely used in automotive air conditioning. R-600a is commonly used in household refrigerators and freezers because of its zero-ozone depletion potential (ODP) and low global warming potential (GWP). R-600a is also known as isobutane. The use of this refrigerant contributes less to climate change. Energy efficiency of refrigeration systems is improved by R-600a's thermodynamic properties. By minimizing energy consumption, it allows effective cooling. Alternative refrigerants tend to be more expensive than isobutane. Manufacturers and consumers alike are attracted to its availability and low cost. Copper and other common refrigeration materials are compatible with R-600a. It can be used in both new and retrofitted equipment. Compared to other refrigerants, R-600a has a

quieter operation. In household appliances such as refrigerators, this can be useful.

Though R-600a is becoming more popular in household refrigeration, especially in Europe and other regions, it is potentially flammable. To ensure safe operation of appliances using R-600a, safety standards and design considerations have been established. To mitigate potential risks associated with the flammability of R-600a, manufacturers implement safety features and use appropriate materials.

2.1 Assumptions

According to the definition of stratified flow, liquids flow down the tube while vapors flow up. When the liquid surface is smooth the flow can be called smoothly stratified. This type occurs at low vapor speeds and when gravity controls the regime. Also, due to low gas velocities, the liquid-vapor interface remains smooth. When the surface is wavy, the vapor velocity increases, and the liquid and vapor interface become unstable. The liquid fills the tube and elongated bubbles appear when the liquid flows intermittently. This type of flow can be divided into plug and slug flow. During the end of the condensation process, this type of flow occurs when the void is small (liquid inventory is large) in combination. The main assumptions used in preparing this model are:

- Equilibrium of flow contain liquid and vapor under the effect of gravity, momentum, pressure gradient, acceleration, interfacial drag, and wall shear.
- The properties of liquid and vapor are in equilibrium with each other during the flow.
- Stable properties for liquid and vapor.
- Tube cross-sections are uniform in length and flow direction.

2.2 Void fraction:

A Gas-Liquid Flow has a void fraction equal to the portion of the tube occupied by gas. This parameter describes how much cross-sectional area is occupied by gas phase in a tube.

The equations above are programmed by EES software based on the integral solution for the quality range 0.95 to 0.05 due to the limitations of the solution. The refrigerants R-134a and R-600a are the recommended refrigerants to be used for charging the refrigerator and freezer and all other home appliances. As confirmed by the standard and the practical, the condensing temperatures are 54.4, 45, 35°C.

Hajal et al.[5] and Thome et al.[14] produced a new definition to the void fraction. Figure 1 depicts as the liquid and gas boundary inside the tube and the top angle of the tube not impregnated with stratified liquid.

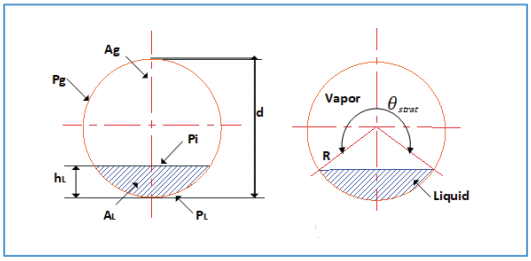

Fig. 1: An analysis of two-phase flow through a circular tube using geometric parameters.

According to the authors, previous research has led to a revised definition of vacuum friction. In this way vacuum friction was defined with a greater degree of precision and accuracy and could represent the gas space very well than the previous model of vacuum friction.

As shown in Fig. 1, the following equations represent two-phase flow in a circular tube.

The homogeneous void fraction:

$$\varepsilon_h = \left[1 + \left(\frac{1-x}{x}\right)\left(\frac{\rho_g}{\rho_l}\right)\right]^{-1} \quad (1)$$

Rouhani and Axelsson void fraction

$$\varepsilon_{ra} = \frac{x}{\rho_g}\left(\left[1 + 0.12(1-x)\left[\frac{x}{\rho_g} + \frac{1-x}{\rho_l}\right] + \frac{1.18(1-x)[g\rho(\rho_l-\rho_g)]^{0.25}}{G\rho_l^{0.5}}\right]\right)^{-1} \quad (2)$$

The logarithmic mean void fraction:

$$\varepsilon = \frac{\varepsilon_h - \varepsilon_{ra}}{ln\left(\frac{\varepsilon_h}{\varepsilon_{ra}}\right)} \quad (3)$$

The start, wavy, mist, and bubbly mass velocity:

$$A_l = A(1-\varepsilon) \quad \rightarrow A_{ld} = \frac{A_l}{di^2}$$

$$A_g = A\varepsilon \quad \rightarrow A_{gd} = \frac{A_g}{di^2}$$

$$\theta_{strat} = 2\pi - 2\left\{\pi(1-\varepsilon) + \left(\frac{3\pi}{2}\right)^{1/3}\left[1 - 2(1-\varepsilon) + (1-\varepsilon)^{1/3} - \varepsilon^{1/3}\right] - \frac{1}{200}(1-\varepsilon)\varepsilon[1-2(1-\varepsilon)][1 + 4(1-\varepsilon)^2 + \varepsilon^2]\right\} \quad (4)$$

$$A_{ld} = \frac{1}{8}[(2\pi - \theta_{strat}) - sin(2\pi - \theta_{strat})] \quad (5)$$

The height of the fluid was determined by the following equations:

$$h_{ld} = 0.5\left(1 - cos\left(\frac{2\pi - \theta_{strat}}{2}\right)\right) \quad (6)$$

The P_{id} geometric expression:

$$P_{id} = sin\left(\frac{2\pi-\theta_{strat}}{2}\right) \quad (7)$$

The G start can be calculated from the below equation:

$$G_{start} = \left\{\frac{(226.3)^2 A_{ld}.A_{gd}^2.\rho_g\,(\rho_l-\rho_g)\mu_l.g}{x^2(1-x)\pi^3}\right\}^{1/3} + 20x \quad (8)$$

According to a study by Nitheanandan et al.[11] and Nitheanandan and Soliman[12], the study uses non-dimensional numbers like Fr and We to view and fix the position of change of the flow patterns from S to SW or from SW to PL or SL flow:

The superficial vapor Reynolds number:

$$Re_{sg} = \frac{x.G.D_i}{\mu_g}$$

The superficial liquid Reynolds number:

$$Re_{sl} = \frac{(1-x).G.D_i}{\mu_l}$$

The parameter of Lockhart- Martinelli:

$$X_{tt} = \left[\frac{1-x}{x}\right]^{0.9} \cdot \left[\frac{\rho_g}{\rho_l}\right]^{0.5} \cdot \left[\frac{\mu_l}{u_g}\right]^{0.1}$$

The two-phase pressure drop multiplier:

$$\emptyset_g = 1 + 1.09X_{tt}^{0.039}$$

Galileo number:

$$G_a = \frac{9.81D_i^3}{\left[\frac{\mu_l}{\rho_l}\right]^2}$$

Froude number:

$$Fr = 1.26 \cdot Re_{ls}^{1.5} \cdot \left[\frac{\emptyset_g}{X_{tt}}\right]^{1.5} \cdot \frac{1}{Ga^{0.5}} \quad \text{for } Re_{sl} > 1250 \quad (9)$$

Weber number:

$$We = 0.85 \cdot Re_{sg}^{0.79} \cdot \left[\frac{\mu_g^2}{\rho_g \cdot D_i \cdot \sigma}\right]^{0.3} \cdot \left[\frac{1}{\emptyset_g}\right]^{0.4} \cdot \left[\left(\frac{\mu_g}{\mu_l}\right)^2 \cdot \frac{\rho_l}{\rho_g}\right]^{0.084} \cdot X_{tt}^{0.157} \quad \text{for } Re_{sl} > 1250 \quad (10)$$

$$G_{wavy} = \left\{\frac{16 \cdot A_{gd}^3 \cdot g \cdot D_i \cdot \rho_l \cdot \rho_g}{x^2 \cdot \pi^2 \cdot (1-(2h_{ld}-1)^2)^{0.5}} \left[\frac{\pi^2}{25h_{ld}^2} \cdot \left(\frac{We}{Fr}\right)^{-1.023} + 1\right]\right\}^{0.5} + 50 - 75 \cdot e^{-(x^2-0.97)^2/x(1-x)} \quad (11)$$

$$G_{mist} = \left\{\frac{7680\, A_{gd}^2\, g\, D_i\, \rho_l\, \rho_g}{x^2\, \pi^2 \zeta} \left(\frac{Fr}{We}\right)\right\}^{0.5} \quad \text{Where}$$

$$\zeta = \left[1.138 + 2\, log\left(\frac{\pi}{1.5A_{ld}}\right)\right]^{-2} \quad (12)$$

$$G_{bubbly} = \left\{\frac{256\, A_{gd}\, A_{gd}^2\, D_i^{1.25} \rho_l\, (\rho_l-\rho_g) g}{0.3164\, (1-x)^{1.75} \pi^2 P_{ld}\, \mu_l^{0.25}}\right\}^{1/1.75} \quad (13)$$

The intermittent to annular flow transition quality:

$$x_{IA} = \left\{\left[0.2914 \left(\frac{\rho_g}{\rho_l}\right)^{-1/1.75} \left(\frac{\mu_l}{\mu_g}\right)^{-1/7}\right] + 1\right\}^{-1} \quad (14)$$

3. Results and discussion

Figure 2 shows the relation between mass velocity and start mass velocity via the quality of the refrigerant R-134a. It also shows the intersection between mass velocity G and start mass velocity G_{start} for different refrigerant flow rates. Condensation temperature is 54.4°C and the inner diameter is 3.25mm. At low refrigerant flow rates (1, 1.5, 2.5) kg.hr^{-1}, there is no intersection between the mass velocity G and the start mass velocity G_{start}, but when the flow increases the intersection is happening. The first intersection occurs when the flow rate is greater than 2.5 kg.hr^{-1} in two points at quality values 0.8-0.4, which consists of flow rates 3.25 kg.hr^{-1} and 4 kg.hr^{-1}. As a result, the pattern changes from S to SW, based upon the limitations in the previous studies that are presented in Table 4. There was a second intersection at the end of the condensation when the quality was between 0.15-0.05. This could be a result of the change in flow pattern from SW to PL flow, as cited in the literature. When the flow rate of the refrigerant reaches higher than 5 kg.hr^{-1}, the intersection occurs at one point for the change from S to SW, and the intersection remains constant until the end of condensation.

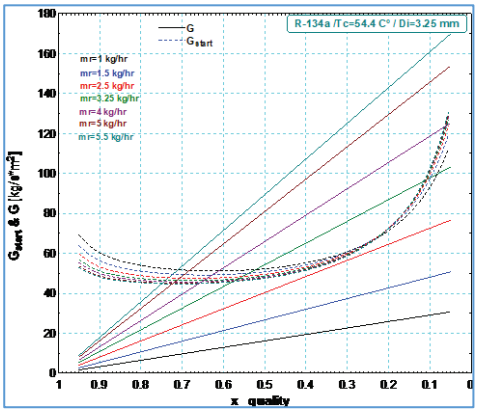

Fig. 2: The mass velocity and start mass velocity using R-134a, at condenser temperature 54.4 °C, and internal diameter 3.25 mm.

Figure 3 has the same trend as Fig. 2 but the inner diameter is 4.826 mm. The trends of the start mass velocity G_{start} were close to the line of the mass velocity G at the higher refrigerant mass flow rate. According to the results, it can be seen that no intersection happened between the mass velocity G and the start mass velocity G_{start}, the flow pattern was not changed from S to SW, and remained S. The effect of the diameter is clear in the behavior of Fig. 2. The increase in the inner diameter maintains the condensation temperature and the type of refrigerant should remain the type of the stratified continuous flow structure.

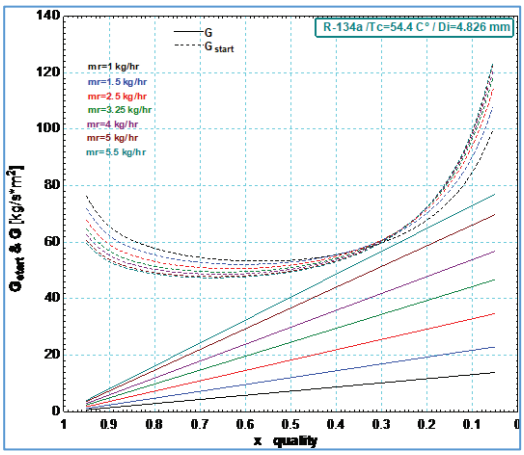

Fig. 3: The relation between the mass velocity and start mass velocity via the quality for R- 134a, condenser temperature 54.4 °C, and internal diameter 4.826 mm.

For 6.299 mm inner tube diameter, Fig. 4 looks like Fig. 3, but the curves of the start mass velocity G start are far from the lines of the start mass velocity G, and there is no intersection between G and G start, so the flow is stratified for different refrigerant flow rates when G < G_{start} as in references[9, 10].

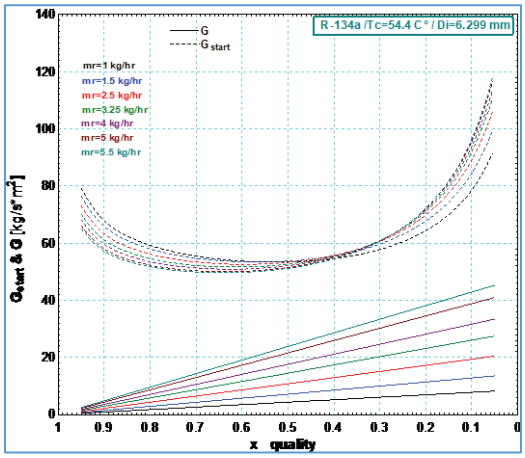

Fig. 4: The relation between the mass velocity and start mass velocity via the quality for R- 134a, condenser temperature 54.4°C, and internal diameter 6.299 mm

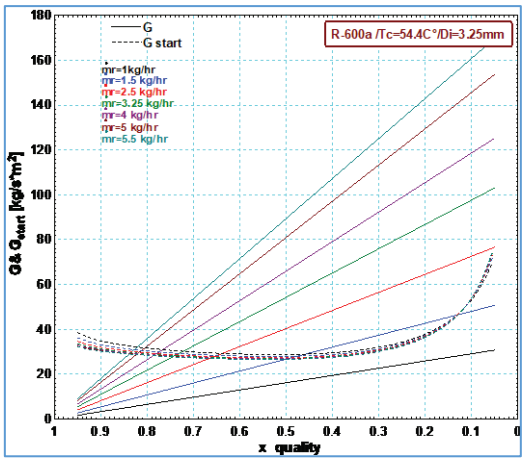

Fig. 5: The relation between the mass velocity and start mass velocity via the quality for R-600a, condenser temperature 54.4 °C, and internal diameter 3.25 mm.

Figure 1A, 2A, 3A, 4A, 5A, and 6A in appendix A provide the relationships between mass velocity and start mass velocity for R-134a at condensing temperatures of 45 and 35°C and for three tube inner diameters of 3.25, 4.826, and 6.299 mm.

The effects of variable refrigerant flow inside the tube when the condensing temperature is 54.4 °C for refrigerant R-600a are shown in Fig. 5.

The change of the flow pattern starts when the flow is greater than 1 $kg.hr^{-1}$ for inner diameter 3.25 mm. The most significant point is change done from S-to-SW flow for R-600a at flow rate 1.5 kg.hr-1 and higher, while starting higher than 2.5 $kg.hr^{-1}$ for R-134a in comparison as presented in Fig. 2.

According to Fig. 6, With R-134a at condensing temperatures of 54.4°C and mass flow rates exceeding 2.5 $kg.hr^{-1}$, the flow rate changes when the diameter of the condenser is equal to or greater than 4.826 mm.

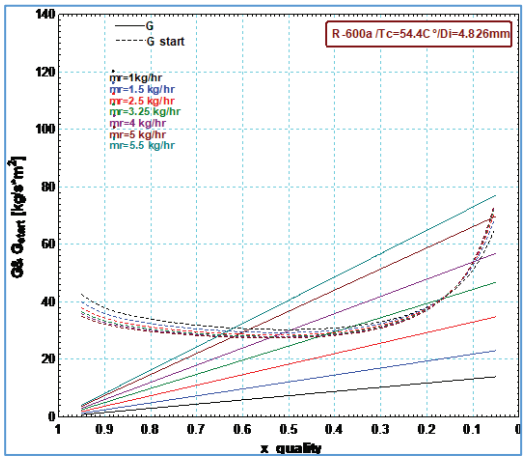

Fig. 6: The relation between the mass velocity and start mass velocity via the quality for R-600a, condenser temperature 54.4 °C, and internal diameter 4.826 mm.

In Fig. 7, it was found that the flow pattern did not change, which means there was no intersection between the mass velocity G and the start mass velocity G_{strat}, and only the higher mass flow rate of 5.5 kg.hr^{-1} where the change was made.

See appendix A for Fig. 7A, 8A, 9A, 10A, 11A, and 12A which show the effects of the condensation temperature change for R-600a. the relation between mass velocity and start mass velocity via the quality at condensing temperatures 45, 35 ℃ and for three inner diameters for the tube 3.25, 4.826, and 6.299 mm.

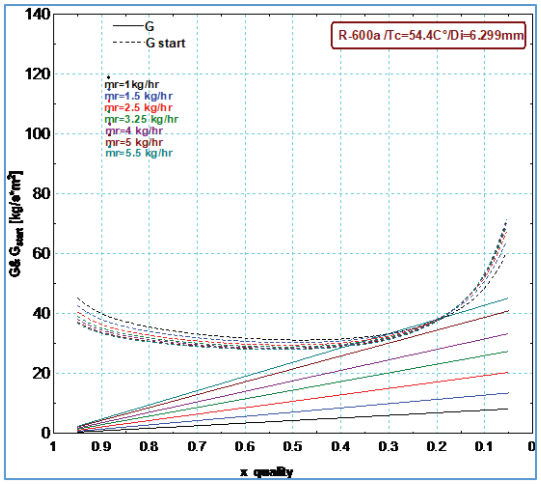

Fig. 7: The relation between the mass velocity and start mass velocity via the quality for R-600a, condenser temperature 54.4 ℃, and internal diameter 6.299 mm.

Figure 8 and 9 show the values of We and Fr numbers at the point of intersection between the G and G_{start} for R-134a and R-600a with different inner tube diameters and condensing temperature. There is an intersection when quality values fall between 0.85 to 0.39 depending on three parameters; the mass flow rate value, the inner tube diameter, and the type of refrigerant. From stratified to stratified wavy, the We number values are 4 to 7 as shown in Fig. 8. The Froude number in Fig. 9 ranges from 2 to 5 at the same quality. The values of We and Fr number are in agreement with findings of the previous studies for the S and SW flow as reported in Nitheanandan et al.[11] and Nitheanandan and Soliman[12], Son et al. [22], and Park et al. [27].

As the inertial force dominates surface tension force for, We and gravitational force dominates as inertial force for Fr number, the gas velocity increases, leading to an increase in We and Fr numbers and causing a change in flow pattern from S to SW.

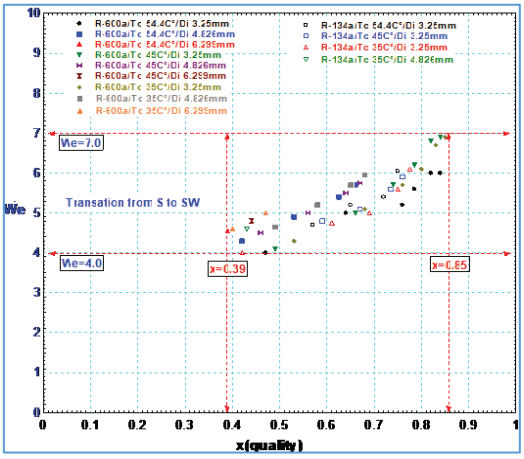

Fig. 8: We Number via the quality for the change from S to SW flow for R-134a &R-600a.

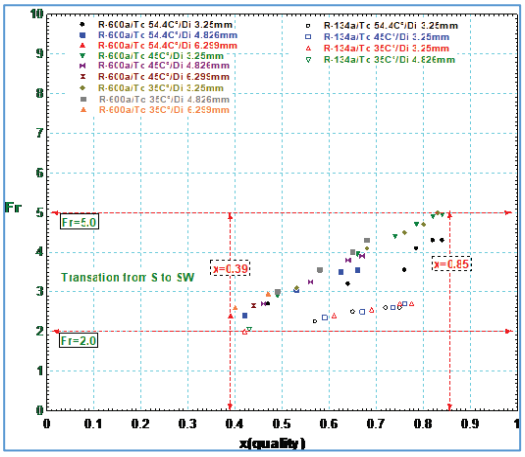

Fig. 9: Fr Number via the quality for the change from stratified to stratified-wavy flow for R-134a &R-600a.

Figure 10 and 11 show that two changes were made to the flow pattern from SW to PL or SL flow, as represented by the numbers of We and Fr for the two refrigerants (R-134a and R-600a) with different inner tube diameters and condensing temperatures. In this model, the value of We and Fr has been changed from 4 to 2 and 2 to 0.4 respectively, and the value of quality started with 0.23 and ended at 0.05. This change was performed at the end of the condensation, as stated by Park et al.[27]. Condensation, according to Park et al.[27], pressure drop and surface tension overcome inertial force causing a decrease in the We number and gravitational force dominating than the inertial force causing the Fr number to decrease and the flow pattern to change to plug or slug flow (internal flow).

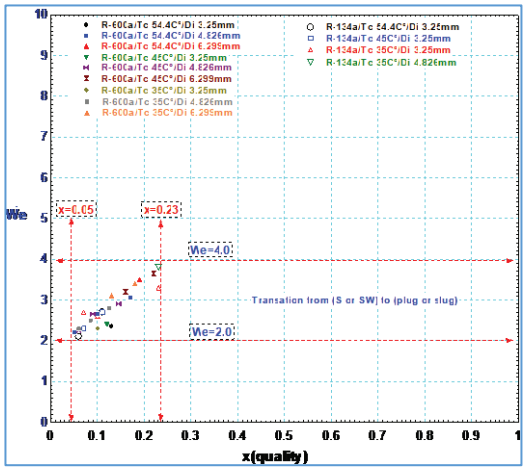

Fig. 10: We Number via the quality for the change from SW or stratified to PL or SL flow for R-134a &R-600a.

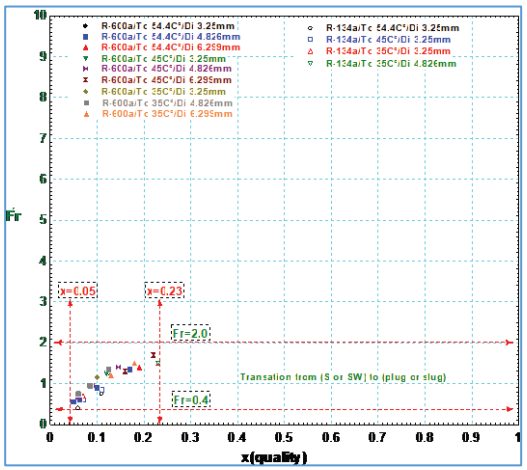

Fig. 11: Fr Number via the quality for the change from SW or S to PL or SL flow for R-134a &R-600a.

Based on the Berber map used for filling study results data, the wavy and stratified flow regime for quality 0.95 to 0.15 is shown in Fig. 12. The end of condensation quality 0.15 to 0.05 is in the slug and plug flow regime.

As with the El-Hajal map, all of the data are displayed in the stratified flow regime, as show in Fig. 13, except for the high mass velocity for the small inner diameter 3.25 mm of three condensation temperatures, which appears in the stratified-wavy regime.

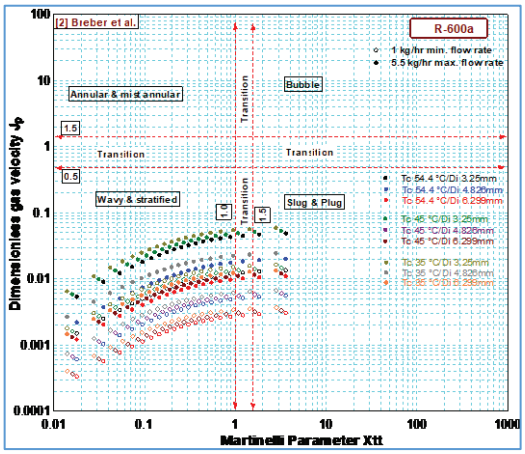

Fig. 12: Comparing the study results with Breber map for R-134a.

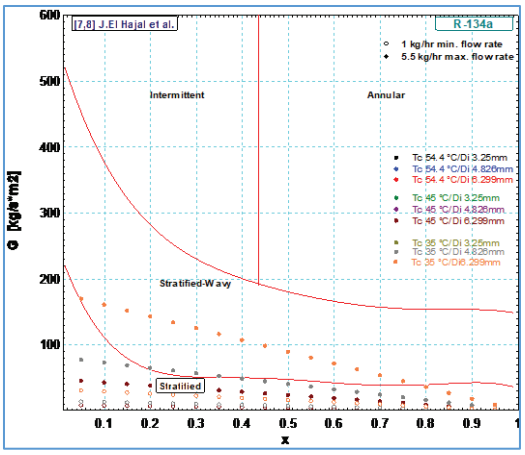

Fig. 13: Comparing the study results with El Hajal map for R-134a.

See Fig. 13A, and 14A for the comparison with Tandon and Taitel maps for R-134a. The same results can be seen in Fig. 14 and Fig. 15 for R-600a.

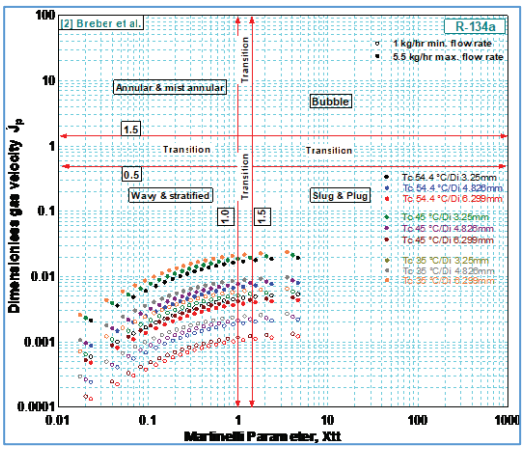

Fig. 14: Comparing the study results with Breber map for R-600a.

Figure 14 confirm the results for R-600a as in Fig.12 which for R-134a. All data fill in S&W rejoin.

Another comparing for the data of R-600a according to Nasr map[31]. All the data fill in stratified rejoin, except for the high mass velocity for the small inner diameter 3.25 that is clear in Fig. 15.

See Fig. 15A, and 16A for the comparing with Tandon and Taitel maps for R-600a.

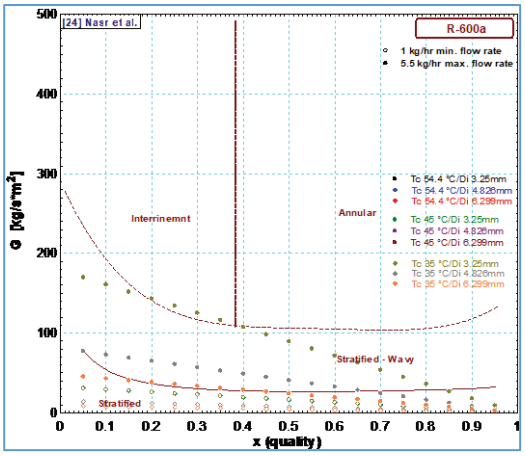

Fig. 15: Comparing the study results with Nasr map [32] for R-600a.

4. Conclusions

According to the integral solution by EES software and the findings results shown in the Figures, the significant points from this study are summarized below:

- The theoretical analysis used in the present study, based on an integration methodology, shows It can detect the transition from stratified flow to stratified wavy flow as well as the transition from SW to PL and SL at the end of condensation.
- The change from SW to PL or SL flow was found at quality 0.15 to 0.05 at the end of condensation for the two refrigerants (R-134a and R-600a).
- Changes from S to SW occur early for small inner diameters and later for larger inner diameters depending on the value of the mass velocity for the two refrigerants (R-134a and R-600a).
- The effect of the refrigerant type showed that the change in flow pattern from S to SW can be observed with R-600a when the diameter of the tube is 4.826 mm. However, it is not noticeable with R-134a when the diameter of the tube is the same It is concluded that the Fr and We Number can be used to clarify the beginning of the change of the flow pattern from S to SW. The obtained values for Fr and We are 2-5 and 4-7, respectively, at quality 0.8 to 0.39.
- The numbers of Fr and We can be used to show the change at the end of the condensation from SW to SL or PL flow. The values of Fr are 2-0.4 and We 4-2 at quality 0.15-0.05, which are in agreement with Nitheanandan et al.[11] and Nitheanandan and Soliman[12] as presented in Table 7 for the two refrigerants (R-134a and R-600a).
- It was found that the condensation temperature had no effect on the change of the flow from S to SW or PL to SL. This was true for different inner diameters and refrigerant types

Table 7: limitations of Nitheanandan et al.[11] and this study

Flow type	We	Fr	$\frac{x^2G^2}{\rho_g}$ (kg.m^{-1}.s^{-2})	Ref.
Mist (M)	≥40	≥7	>100	Nitheanandan et al. [11]
Annular (A)	<40	≥7	>100	Nitheanandan et al. [11]
Transition from wavy annular to wavy (WA-W)		=18		Nitheanandan et al. [11]
Wavy (W)	-	<7	-	Nitheanandan et al. [11]
Stratified to stratified wavy	4-7	2-5		This study
Stratified to internment	4-2	2-0.4		This study

Nomenclature

A	"Area (m^2)"
D_i	"Internal diameter (m)"
f	"Friction factor"
Fr	"Froude number"
g	"Gravity (m.s^{-2})"
G	"Mass velocity (kg.s^{-1}.m^{-2})"
Ga	"Galileo number"
G_{strat}	"Stratified mass velocity (kg.s^{-1}.m^{-2})"
G_{wavy}	"Wavy mass velocity (kg.s^{-1}.m^{-2})"
G_{mist}	"Mist mass velocity (kg.s^{-1}.m^{-2})"
G_{bubbly}	"Bubbly mass velocity (kg.s^{-1}.m^{-2})"
h_{Ld}	"Dimensionless liquid Height"
J_g^*	Wallis dimensionless gas velocity
L	Length (m)
$\dot{m}_r$	Refrigerant flow rate (kg. s^{-1})
P	Pressure (Pa)
P_{id}	Dimensionless perimeter of interface

Re	Reynold number
T	Temperature (℃)
v	Specific volume ($m^3 \cdot kg^{-1}$)
We	Weber number
x	Quality
Xtt	Lockhart-Martinelli parameter

Greek symbols

ε	"Logarithmic mean void fraction"
ε_h	"Homogenous void fraction"
ε_{ra}	"Rouhani and Axelsson void fraction"
μ	"Dynamic viscosity ($N.s.m^{-2}$)"
θ	"Upper angle of the tube not wetted by stratified liquid (rad)"
θ_{strat}	"Stratified angle around upper perimeter of the tube (rad)"
ρ	"Density ($Kg.m^{-3}$)"
Ø	"Tow-phase pressure drop multiplier"

Subscripts

ci	"Cross section inside"
g	"Gas"
l	"Liquid"
f	"Friction"

References

1) M.I. Alhamid, N. Nasruddin, E. Susanto, T.F. Vickary, M.A. Budiyanto, "Refrigeration cycle exergy-based analysis of hydrocarbon (R600a) refrigerant for optimization of household refrigerator, *EVERGREEN Joint Journal of Novel Carbon Resource Sciences & Green Asia Strategy*, 06 (01) 71-77 (2019).
2) A. Pal, K. Uddin, K. Thu, B.B. Saha, "Environmental assessment and characteristics of next generation refrigerants", *EVERGREEN Joint Journal of Novel Carbon Resource Sciences & Green Asia Strategy*, 05 (02) 58-66 (2018).
3) S. A. Shaedi, N. Mohd-Ghazali, J-T Oh, R. Ahmad, Y. Mod-Yunos, "Entropy generation minimization of two-phase flow in a mini channel with genetic algorithm", *EVERGREEN Joint Journal of Novel Carbon Resource Sciences & Green Asia Strategy*, 06 (1) 39-43 (2019).
4) A.S. Pamitran, S. Novianto, N. Mohd-Ghazali, R.A. Koestoer, "Flow pattern of two-phase flow boiling with heat transfer and pressure drop using natural refrigerant (propane) in microchannel", *EVERGREEN Joint Journal of Novel Carbon Resource Sciences & Green Asia Strategy*, 7 (4) 544-548 (2020). doi.org/10.5109/4150474
5) J. El Hajal, J.R. Thome, A. Cavallini, "Condensation in horizontal tubes, part 1: Two-phase flow pattern map", *International Journal of Heat and Mass Transfer*, 46 (18) 3349–3363 (2003). https://doi.org/10.1016/S0017-9310(03)00139-X
6) A.H. Al-Zaidi, M.M. Mahmoud, T.G. Karayiannis, "Condensation flow patterns and heat transfer in horizontal microchannels". *Experimental Thermal and Fluid Science*, 90 153–173 (2018). https://doi.org/10.1016/j.expthermflusci.2017.09.009
7) H. Han, M. Hatta, H. Rahman, "Smart ventilation for energy conservation in buildings", *EVERGREEN Joint Journal of Novel Carbon Resource Sciences & Green Asia Strategy*, 06 (01) 44-51 (2019).
8) Y. Taitel, A.E. Dukler, "A model for predicting flow regime transitions in horizontal and near horizontal gas-liquid flow", *AIChE Journal*, 22 (1) 47–55 (1976). https://doi.org/10.1002/aic.690220105
9) G. Breber, J.W. Palen, J. Taborek, "Prediction of horizontal tube side condensation of pure components using flow regime criteria," *Journal of Heat Transfer*, 102 (3) 471–476 (1980). https://doi.org/10.1115/1.3244325
10) N.T. Tandon, H. K. Varma, C. P. Gupta, "A new flow regimes map for condensation inside horizontal tubes", *Journal of Heat Transfer*, 104 (4) 763–768 (1982). https://doi.org/10.1115/1.3245197
11) T. Nitheanandan, H.M. Soliman, R.E. Chant, "A proposed approach for correlating heat transfer during condensation inside tubes" *ASHRAE transaction*, 96 (Part 1) 230-241 (1990).
12) T. Nitheanandan, H.M. Soliman, "Influence of tube inclination on the flow regime boundaries of condensing steam", *The Canadian Journal of Chemical Engineering*, 71 (1) 35–41, (1993). https://doi.org/10.1002/cjce.5450710106
13) M.K. Dobson, J. C. Chato, "Condensation in smooth horizontal tubes", *Journal of Heat Transfer*, 120 (1) 193–213 (1998). https://doi.org/10.1115/1.2830043
14) J. R. Thome, J. El Hajal, A. Cavallini, "Condensation in horizontal tubes, part 2: New heat transfer model based on flow regimes", *International Journal of Heat and Mass Transfer*, 46 (18) 3365–3387 (2003). https://doi.org/10.1016/S0017-9310(03)00140-6
15) D. Jung, K.H. Song, Y., Cho, S.J. Kim, "Flow condensation heat transfer coefficients of pure refrigerants", *International Journal of Refrigeration*, 26 (1) 4–11 (2003). https://doi.org/10.1016/S0140-7007(02)00082-8
16) A. Cavallini, "Enhanced Heat Transfer in Internal Condensation of Refrigerants". The Institute of Refrigeration 1–15 (2004).
17) S. Koyama, J. Lee, R. Yonemoto, "An investigation on void fraction of vapor-liquid two-phase flow for smooth and micro fin tubes with R134a at adiabatic condition", *International Journal of Multiphase Flow*, 30 (3) 291–310 (2004).

https://doi.org/10.1016/j.ijmultiphaseflow.2003.10.009

18) J.R. Thome, "Condensation in plain horizontal tubes: Recent advances in modelling of heat transfer to pure fluids and mixtures", *Journal of the Brazilian Society of Mechanical Sciences and Engineering*, 27 (1) 23–30 (2005). https://doi.org/10.1590/S1678-58782005000100002
19) D. Del Col, A. Cavallini, J.R. Thome, "Condensation of zeotropic mixtures in horizontal tubes: New simplified heat transfer model based on flow regimes", *Journal of Heat Transfer*, 127 (3) 221–230 (2005). https://doi.org/10.1115/1.1857951
20) E.W. Jassim, T.A. Newell, J.C. Chato, "Prediction of two-phase condensation in horizontal tubes using probabilistic flow regime maps. *International Journal of Heat and Mass Transfer*, 51 (3–4) 485–496 (2008). https://doi.org/10.1016/j.ijheatmasstransfer.2007.05.021
21) R. Suliman, L. Liebenberg, J.P. Meyer, "Improved flow pattern map for accurate prediction of the heat transfer coefficients during condensation of R-134a in smooth horizontal tubes and within the low-mass flux range", *International Journal of Heat and Mass Transfer*, 52 (25–26) 5701–5711 (2009). https://doi.org/10.1016/j.ijheatmasstransfer.2009.08.017
22) C.H. Son, H.S. Lee, "Condensation heat transfer characteristics of R-22, R-134a and R-410A in small diameter tubes", *Heat and Mass Transfer/Waerme-Und Stoffuebertragung*, 45 (9) 1153–1166 (2009). https://doi.org/10.1007/s00231-009-0489-6
23) E. van Rooyen, M. Christians, L. Liebenberg, J.P. Meyer, "Probabilistic flow pattern-based heat transfer correlation for condensing intermittent flow of refrigerants in smooth horizontal tubes", *International Journal of Heat and Mass Transfer*, 53 (7–8) 1446–1460 (2010). https://doi.org/10.1016/j.ijheatmasstransfer.2009.12.005
24) H. Lee, I. Mudawar, M.M. Hasan, "Flow condensation in horizontal tubes", *International Journal of Heat and Mass Transfer*, 66 31–45 (2013). https://doi.org/10.1016/j.ijheatmasstransfer.2013.06.044
25) S.G. Mohseni, M.A. Akhavan-Behabadi, M. Saeedinia, "Flow pattern visualization and heat transfer characteristics of R-134a during condensation inside a smooth tube with different tube inclinations", *International Journal of Heat and Mass Transfer*, 60 (1) 598–602 (2013). https://doi.org/10.1016/j.ijheatmasstransfer.2013.01.023
26) L. Doretti, C. Zilio, S. Mancin, A. Cavallini, "Condensation flow patterns inside plain and micro fin tubes: A review", *International Journal of Refrigeration*, 36 (2) 567–587 (2013). https://doi.org/10.1016/j.ijrefrig.2012.10.021
27) I. Park, H. Lee, I. Mudawar, "Determination of flow regimes and heat transfer coefficient for condensation in horizontal tubes", *International Journal of Heat and Mass Transfer*, 80 698–716 (2015). https://doi.org/10.1016/j.ijheatmasstransfer.2014.09.035
28) S. Saini, J. Thaker, J. Banerjee, "Analysis of interfacial dynamics in stratified and wavy-stratified flow using Laser Doppler Velocimetry", *Experimental and Computational Multiphase Flow*, I (1) 1–14 (2021). https://doi.org/10.1007/s42757-020-0083-1
29) V. Sereda, V. Rifert, V. Gorin, O. Baraniuk, P. Barabash, "Heat transfer during film condensation inside horizontal tubes in stratified phase flow", *Heat and Mass Transfer/Waerme- Und Stoffuebertragung*, 57 (2) 251–267 (2021). https://doi.org/10.1007/s00231-020-02946-2
30) Mahdi, L. A. A. A., Fayad, M. A., & Chaichan, M. T. (2023). In Tube Condensation: Changing the Pressure Drop into a Temperature Difference for a Wire-on-Tube Heat Exchanger. *Fluid Dynamics and Materials Processing*, *19*(9), 2201–2214. https://doi.org/10.32604/fdmp.2023.027166
31) M. Nasr, M.A. Akhavan-Behabadi, M. R. Momenifar, P. Hanafizadeh, "Heat transfer characteristic of R-600a during flow boiling inside horizontal plain tube", *International Communications in Heat and Mass Transfer*, 66 93–99 (2015). https://doi.org/10.1016/j.icheatmasstransfer.2015.05.024.

Appendix A:

There is no change for flow behavior when the condenser temperature is 45 ℃ for R-134a as in Fig. A1, A2, and A3. Also, when the condenser temperature 35 °C as in Fig. A4, A5, and A6. This means no effect for the condensing temperature about the type of the flow pattern or the change from stratified-to-stratified wavy flow.

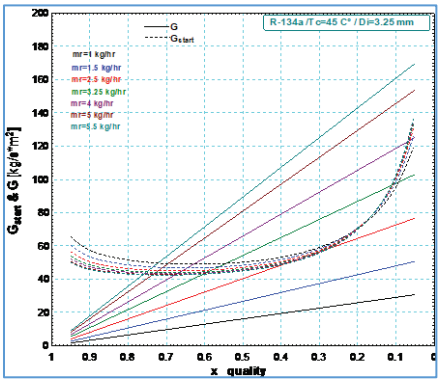

Fig. 1A: The mass velocity and start mass velocity via the quality for R-134a, condenser temperature 45°C, and internal diameter 3.25.

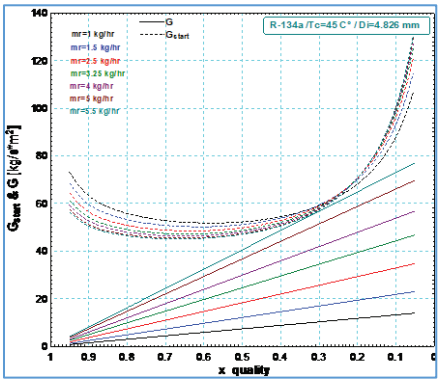

Fig. 2A: The mass velocity and start mass velocity via the quality for R-134a, condenser temperature 45°C, and internal diameter 4.826 mm.

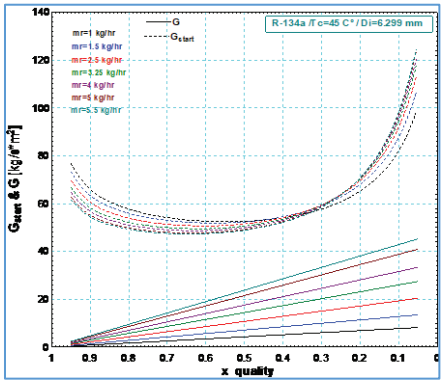

Fig. 3A: The mass velocity and start mass velocity via the quality for R-134a, condenser temperature 45°C, and internal diameter 6.299 mm.

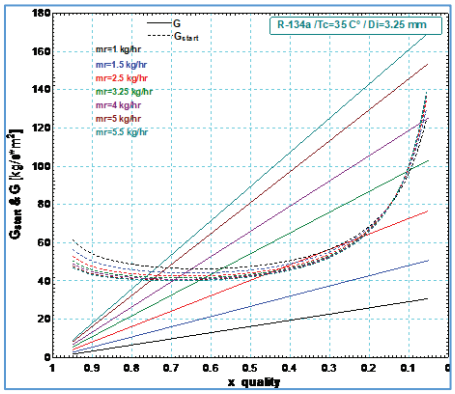

Fig. 4A: The mass velocity and start mass velocity via the quality for R-134a, condenser temperature 35°C, and internal diameter 3.25mm.

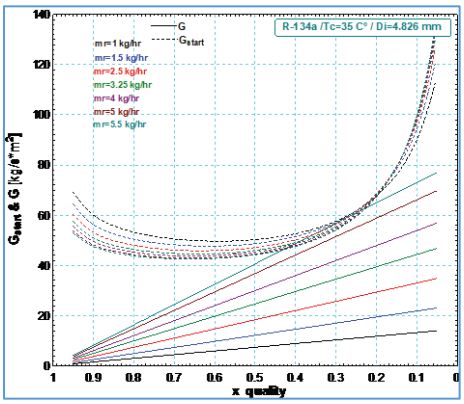

Fig. 5A: The mass velocity and start mass velocity via the quality for R-134a, condenser temperature 35°C, and internal diameter 4.826mm.

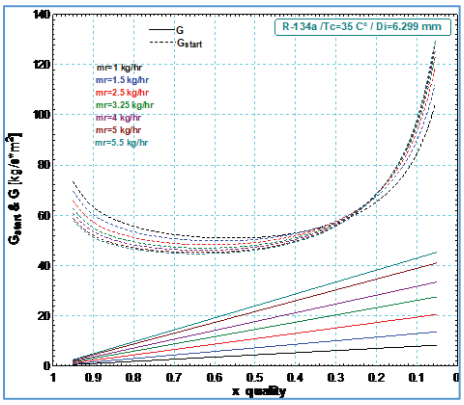

Fig. 6A: The mass velocity and start mass velocity via the quality for R-134a, condenser temperature 35°C, and internal diameter 6.299 mm.

The same trends are found in Fig. 7A, 8A, and 9A for R-600a at condensing temperatures 45 °C. The results from these Figures show the effect of the inner diameter on the change of the flow from S to SW and no effect for the condensing temperature on the behavior of the flow pattern

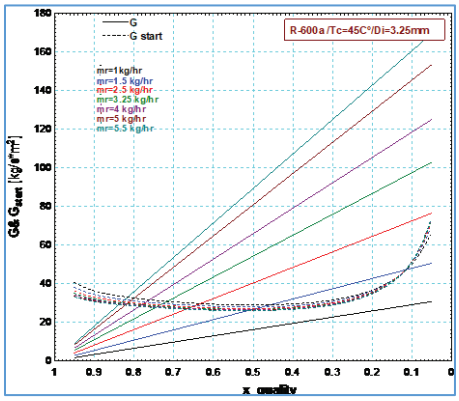

Fig. 7A: The mass velocity and start mass velocity via the quality for R-600a, condenser temperature 45°C, and internal diameter 3.25mm.

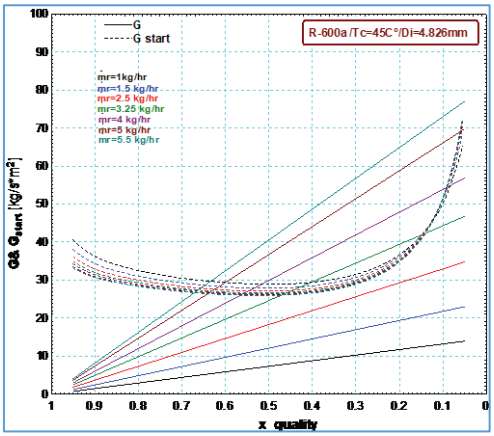

Fig. 8A: The mass velocity and start mass velocity via the quality for R-600a, condenser temperature 45°C, and internal diameter 4.826mm.

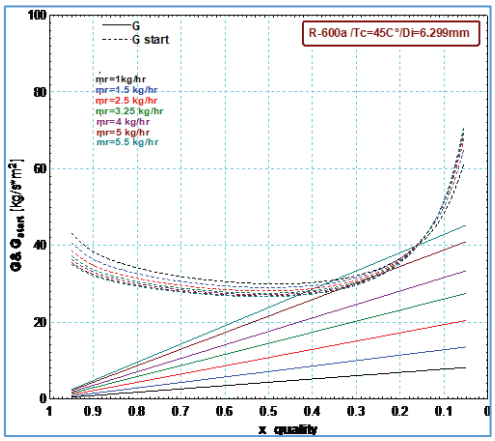

Fig. 9A: The mass velocity and start mass velocity via the quality for R-600a, condenser temperature 45°C, and internal diameter 6.299 mm.

The same trends are found in Fig. 10A, 11A, and 12A for R-600a at condensing temperatures 35 °C. The results from these Figures show the effect of the inner diameter on the change of the flow from S to SW and no effect for the condensing temperature on the behavior of the flow pattern.

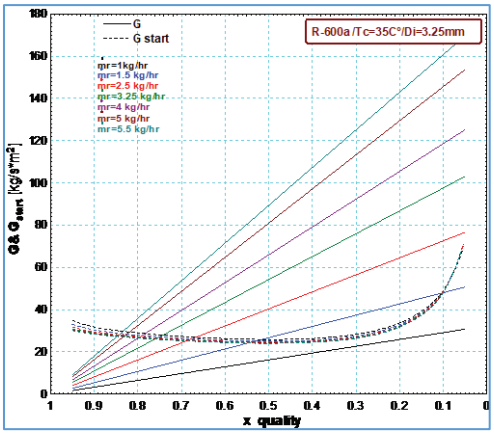

Fig. 10A: The mass velocity and start mass velocity via the quality for R-600a, condenser temperature 35°C, and internal diameter 3.25mm.

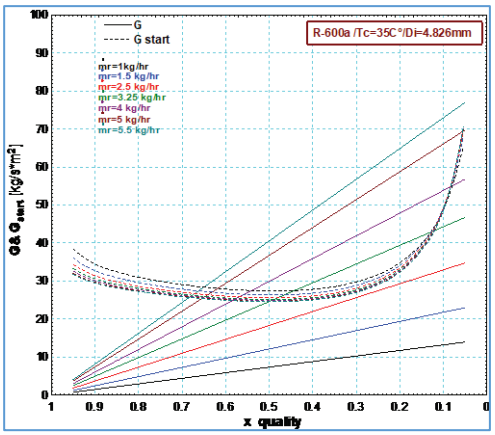

Fig. 11A: The mass velocity and start mass velocity via the quality for R-600a, condenser temperature 35°C, and internal diameter 4.826mm.

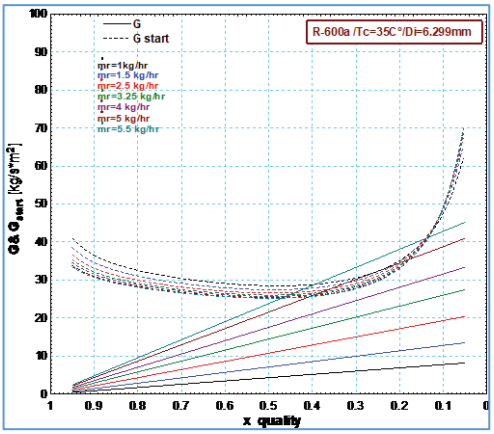

Fig. 12A: The mass velocity and start mass velocity via the quality for R-600a, condenser temperature 35°C, and internal diameter 6.299 mm.

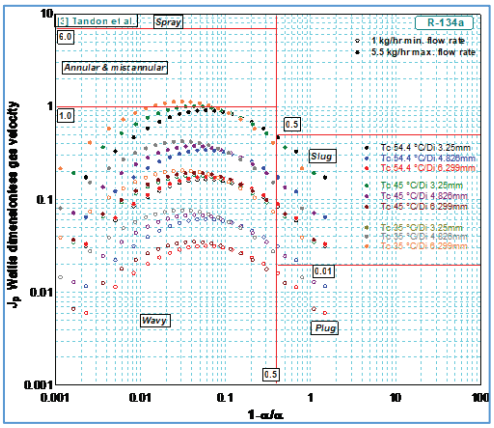

Fig. 13A: Comparing the study results with Tandon map for R-134a.

Figure 13A is the Tandon map, also the results data for this study fill in the wavy regime which consists of the stratified flow and the end of the condensation in slug and plug flow regime. The low mass flow rate data for all condensation temperatures full at the lower part of the wavy regime while the high mass flow rate data approach the annular flow regime.

Figure 14A is Taitel approach and all the results data fill in the gravity flow regime which the heat transfer depending on the temperature difference between the refrigerant and the wall temperature.

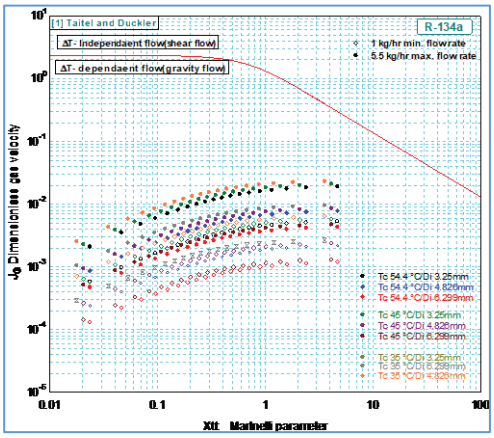

Fig. 14A: Comparing the study results with Taitel Map for R-134a.

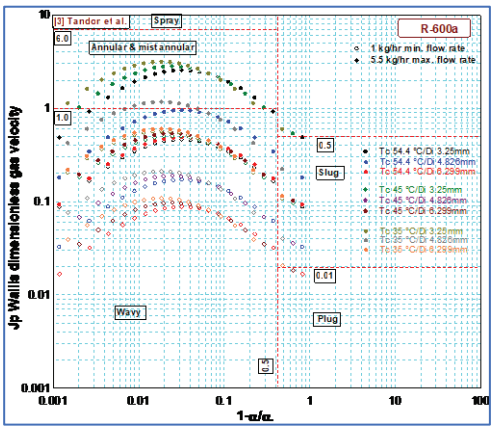

Fig. 15A: Comparing the study results with Tandon map for R-600a.

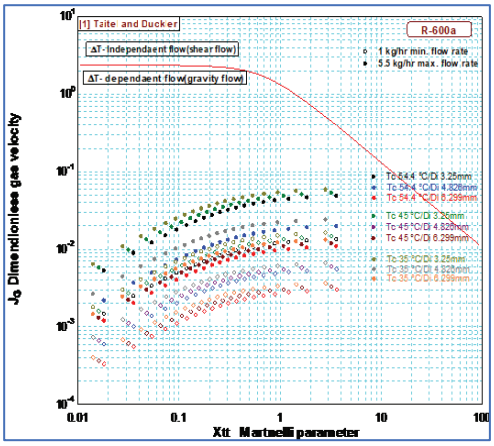

Fig. 16A: Comparing the study results with Taitel map for R-600a.